Durability of FRP reinforcing bars exposed to an alkaline environment with/without additional sustained load

Noëmie Delaplanque, Sylvain Chataigner, Laurent Gaillet, Xavier Bourbon, Marc Quiertant, Karim Benzarti, Arnaud Rolland, Bigaud David

CICE 2023 Rio de Janeiro – Brazil 11TH INTERNATIONAL CONFERENCE ON FRP COMPOSITES IN CIVIL ENGINEERING

DURABILITY OF FRP REINFORCING BARS EXPOSED TO AN ALKALINE ENVIRONMENT WITH/WITHOUT ADDITIONAL SUSTAINED LOAD

Delaplanque Noëmie, Univ Gustave Eiffel, MAST-SMC, F-44344 Bouguenais, France, noemie.delaplanque@univ-eiffel.fr
Chataigner Sylvain, Univ Gustave Eiffel, MAST-SMC, F-44344 Bouguenais, France, sylvain.chataigner@univ-eiffel.fr
Gailler Laurent, Univ Gustave Eiffel, MAST-SMC, F-44344 Bouguenais, France, Laurent.gaillet@univ-eiffel.fr
Bourbon Xavier, Andra, Direction de la recherche et développement, F-92298 Châtenay-malabry, France, xavier.bourbon@andra.fr
Quiertant Marc, Univ Gustave Eiffel, MAST-EMGCU, F-77454 Marne-La-Vallée, France, marc.quiertant@uinv-eiffel.fr
Benzarti Karim, Univ Gustave Eiffel, ENPC, CNRS, Lab Navier, F-77454 Marne-La-Vallée, France, karim.benzarti@univ-eiffel.fr
Rolland Arnaud, Cerema, MAN, F-44200 Nantes, France, Arnaud.rolland@cerema.fr
Bigaud David, Univ Angers, LARIS, SFR MATHSTIC, F-49000 Angers, France, david.bigaud@univ-angers.fr

ABSTRACT

Corrosion of steel reinforcing bars (rebars) is the main cause of degradation of reinforced concrete structures. This issue may be addressed by using corrosion-resistant rebars made of Fiber-Reinforced Polymer (FRP). However, in France, the use of FRP rebars is currently limited to temporary applications due to a lack of comprehensive data on their durability in service conditions. Although many studies have investigated the durability of FRP rebars exposed to different alkaline environments (aiming to simulate the surrounding concrete), little is known about the combined effects of alkali ions and sustained loading.

The use of FRP rebars is an alternative option to steel reinforcements investigated for some structural components in the Cigéo project. Reinforced concrete structures in the deep geological disposal are exposed to degradation by corrosion, but also subjected to aging under temperature (exothermic waste) and load (convergence of the geological environment).

This paper presents preliminary findings from a durability study conducted on Glass FRP (GFRP) and Carbon FRP (CFRP) rebars subjected to alkali environments at different temperatures. Additionally, for some GFRP specimens, sustained tensile loading was applied at 20% and 40% of the tensile strength. The study included mechanical, physico-chemical, and microstructural characterizations of the various series of aged rebars. The experimental data obtained were subsequently analysed to assess the potential influence of sustained load on the degradation kinetics of GFRP rebars.

This ongoing study is a collaborative effort between Gustave Eiffel University and the French National Agency for Nuclear Waste Management (Andra), aligned with the recent guidelines published by the French Civil Engineering Association (AFGC).

KEYWORDS

Durability; FRP rebars; Alkaline solution; Concrete; Sustained load.

INTRODUCTION

To address the issue of corrosion affecting steel reinforcements in concrete structures, an effective solution is the substitution of steel with Fiber-Reinforced Polymer (FRP) reinforcing bars (rebars). Unlike steel, FRPs are not susceptible to corrosion and offer higher mechanical strength. However, the

adoption of FRP rebars in France remains limited, mainly due to insufficient data regarding their long-term durability under service conditions (Souchu, 2009).
While numerous studies have explored the durability of Glass FRP (GFRP) rebars exposed to alkaline environments, limited information is available regarding the combined effects of environmental exposure and mechanical stresses (AFGC, 2021). However, several studies have highlighted that the application of a sustained load (creep) significantly impacts the degradation kinetics of FRP rebars in aggressive environments.
For instance, (Byars et al., 2019) conducted a study focusing on GFRP and Carbon FRP (CFRP) rebars. Their findings demonstrated that the application of a sustained load (ranging from 20% to 40% of the rebar's tensile strength), along with accelerated aging (at temperatures of 23°C, 40°C, and 60°C), further accelerates the degradation kinetics of the rebars in an alkaline medium. Moreover, the study demonstrated that GFRP rebars are more susceptible to these aging conditions compared to CFRP rebars.
This article presents the preliminary findings of a study investigating the impact of mechanical loading combined with accelerated aging on the degradation kinetics of GFRP rebars. The first part of the article introduces the experimental program, while the second part presents findings regarding the evolution of both mechanical and physico-chemical properties of GFRPs when exposed to accelerated aging without the application of mechanical loading (for various periods up to 360 days). The final section is dedicated to the evaluation of the rebars after aging under mechanical stress. It is important to note that the experimental program discussed in this article is still currently in progress.

EXPERIMENTAL PROGRAM

Presentation of the studied FRP rebars

This study investigates the durability of FRP rebars available on the market, which are composed of a vinylester matrix reinforced with either glass fibers (GFRP) or carbon fibers (CFRP). These rebars were manufactured through the pultrusion process. The rebars have a diameter of 10mm and a sandcoated surface finish, as illustrated in Figure 1. Table 1 provides the key properties of these FRP rebars as supplied by the manufacturer.

a) CFRP rebar b) GFRP rebar

Figure 1 : Surface finishes of the two FRP rebars considered in this study

Table 1 : Properties of GFRP and CFRP rebars supplied by the manufacturer

Rebars	Nominal diameter (mm)	Effective surface area (mm^2)	Guaranteed tensile strength (MPa)	Modulus of elasticity in tension (GPa)
GFRP	10	71	900	46
CFRP	10	71	2000	150

Characterization methods

In the framework of this durability study, the rebars were characterized both in the initial state and after aging, in order to assess any evolution of their mechanical and physico-chemical properties over aging.

The tensile strength and the longitudinal modulus of elasticity of the rebars were determined through tensile tests conducted in accordance with the American standard ASTM D7205 (ASTM, 2006), the ISO standard 10406-1 (ISO, 2008) and the French AFGC recommendations (AFGC, 2021). To prevent excessive damage to the ends of the FRP rebars during testing and to avoid premature rupture, a specific anchoring system was employed at each end. This system consisted of a steel tube filled with expansive mortar, which enabled more uniform distribution of radial tightening stresses. The tensile tests were performed on a hydraulic universal testing machine (UTM) of capacity 250 kN equipped with a force

measurement cell, at a displacement rate of 1 mm/min (see Figure 2.a). To measure the strain of the rebar during loading, a non-contact video extensometer was employed. This setup ensured accurate and reliable data collection during the experiments.
Interlaminar shear tests, known as short-beam tests, were also conducted on the FRP rebars in accordance with the ASTM D4475 standard (ASTM, 2006) and the AFGC recommendations (AFGC, 2021). This method involves subjecting the rebar to a three-point bending test with closely spaced supports (Figure 2.b) and enables the assessment of the interface strength between the fibers and the polymer matrix. The distance between supports was set at five times the diameter of the FRP rebar. The short-beam test was performed using an electromechanical UTM of capacity 100 kN, at a displacement rate of 1mm/min. To enable more accurate force measurement within the strength range of the study, the UTM was equipped with a 50 kN load cell. This configuration ensured precise and reliable force measurements during the testing process. The interlaminar shear strength (R) was determined using the formula specified in the ASTM test standard (ASTM, 2002), where $R = 0.849F/d^2$. Here, F represents the breaking force, and d corresponds to the diameter of the FRP rebar.

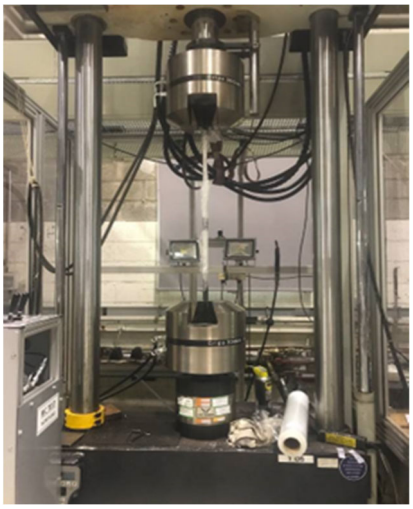

a) Tensile test

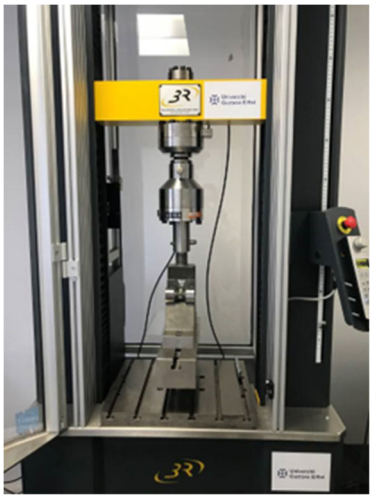

b) Short-beam test

Figure 2 : Experimental setups used for the mechanical tests

In addition to the previous mechanical tests, various physico-chemical characterizations were conducted on the FRP rebars before and after the aging process. These characterizations included Differential Scanning Calorimetry (DSC) analysis to evaluate the glass transition temperature of the polymer matrix, Fourier Transform Infrared (FTIR) spectroscopy to monitor any potential evolution of the chemical structure of the FRP material during aging, as well as Scanning Electron Microscopy (SEM) observations. However, in this paper, only the results of the DSC analyses are presented. The DSC experiments were performed using a TA Instruments DSC 250 calorimeter operating in the temperature modulation mode (MDSC). The glass transition temperature of the FRP samples (~20 mg taken from the core of the rebars) was measured during a heating ramp from 20°C to 250°C, at a rate of 3°C/min and with a superimposed temperature modulation of amplitude of 1.5°C and a period of 60s.

Accelerated aging in alkaline environments without mechanical stress

As mentioned earlier, a series of FRP rebars were subjected to accelerated aging in alkaline environments without the application of additional mechanical stress. This specific aging condition is denoted as ANL (Aging with No Load applied) in the following sections. The FRP rebars were first embedded in a concrete cylinder with a 50mm external diameter. These specimens were then immersed in an alkaline solution, which consisted of sodium hydroxide (NaOH) at a concentration of 0.1 mol/L and potassium hydroxide (KOH) at a concentration of 0.5 mol/L, resulting in a pH level of around 13.5. This solution is commonly employed in durability studies (Rolland, 2021) due to its ability to simulate the concrete medium at early age. GFRP rebars were immersed in large tanks filled with this alkaline solution and regulated at three different temperatures: 20°C (room temperature), 40°C, and 60°C

(Figure 3a). Differently, CFRP specimens were only exposed to the solution at 60°C (i.e., the most severe condition).
After different periods of exposure (E1= 30 days, E2 = 60 days, E3 = 90 days, E4 = 180 days, E5 = 360 days), the specimens were removed from the baths to undergo mechanical and physico-chemical characterization using the methods introduced earlier. The concrete cover around the FRP specimens was removed prior to the characterizations.

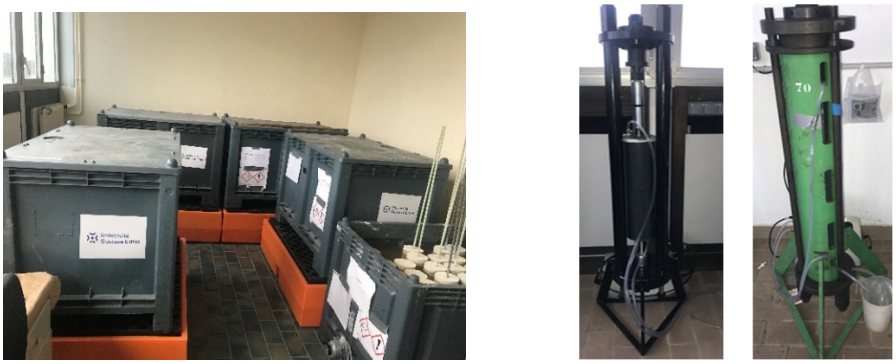

a) b)

Figure 3 : a) Conditioning of ANL specimens in thermoregulated tanks filled with the alkaline solution; b) Metallic devices used for exposing the FRP specimens to an alkaline environment combined with sustained load (ASL conditions)

Accelerated aging in alkaline environments in combination with sustained load

Another set of GFRP specimens embedded in concrete cylinders was exposed to alkaline environments combined with sustained load, designated as ASL conditions (Aging under Sustained Load) in the following. It is to note that CFRPs were not tested under these conditions.

For this purpose, two models of metallic devices were utilized, as depicted in Figure 3b, with a total of six devices allowing for the simultaneous exposure of six specimens. These devices enabled the specimens to be loaded using a hydraulic jack, and the resulting longitudinal deformation was then maintained by securing the anchors. To ensure a constant force during aging, a reloading procedure was implemented due to relaxation phenomena. This procedure was calibrated using preliminary specimens that were monitored using a load cell. Maintaining constant force is a crucial aspect of these investigations, particularly considering the significant relaxation that can occur, especially at elevated temperatures. Using this device, two levels of load were examined, corresponding to 20% and 40% of the average tensile strength of the unaged FRP rebars (as determined at 20°C).

Besides, each device was equipped with a double cell: one cell containing the alkaline solution and the other for circulating water at a fixed temperature. Here again, three different temperatures were used, namely 20°C, 40°C, and 60°C. The specimens were aged for periods of up to 90 days under these ASL conditions.

Optimizing the design of experiments under ASL conditions

To minimize the overall duration of the aging campaign under ASL conditions, which involves a substantial number of specimens, an optimized design of experiments was implemented. This design is based on the concept of Hoke matrices, utilizing two variable factors: temperature and load. The advantage of this strategy is the reduction in the number of test combinations while still retaining valuable information for studying the coupling of aging parameters.

An example of this optimized design is matrix D1, represented by the blue points in Figure 4. This matrix effectively captures the essential aspects of the coupling of aging parameters. To ensure comprehensive coverage, an additional configuration was introduced at 40°C without applied load, represented by the red point in Figure 4 (configuration #7). This inclusion enables a more comprehensive understanding of the effects of temperature and load on the aging process, providing a more robust analysis of the specimens' behavior.

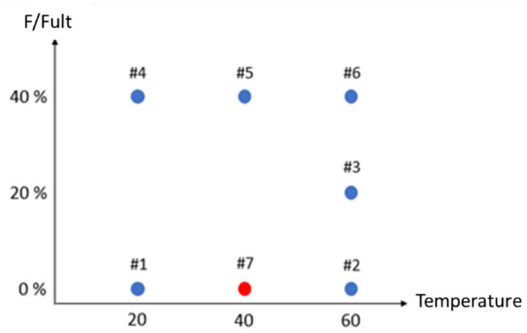

Figure 4 : Optimized design of experiments for the ASL test campaign

PRELIMINARY RESULTS UNDER ANL AGING CONDITIONS (WITHOUT LOAD)

Impact of ANL conditions on the tensile properties of the FRP rebars

Tensile tests were conducted on FRP specimens aged for the various durations under ANL conditions, in order to evaluate their residual properties. The failure modes commonly observed for GFRP and CFRP rebars are depicted in Figure 5. GFRPs typically undergo a brittle failure, whereas CFRPs exhibit more localized failure occurring at various points along the test device. These localized ruptures were observed to initiate primarily in the center of the rebar and subsequently near the anchorages, probably due to the release (after the first failure) of the elastic energy stored during loading.

Figure 5: Typical tensile failure modes of GFRP (bottom) and CFRP (top) rebars, after exposure to ANL conditions.

The average tensile strength and longitudinal modulus of elasticity of the aged rebars are presented in Table 2, while their variations over time (at different temperatures for GFRPs and at 60°C only for CFRPs) are illustrated in Figures 6 and 7, respectively. The modulus of elasticity was determined using the following equation:

$$E = \frac{\sigma_{40\%} - \sigma_{20\%}}{\varepsilon_{40\%} - \varepsilon_{20\%}}$$

With E, the longitudinal modulus of elasticity, σ, the stress of rebars at 20 and 40% of the tensile strength, and ε, the strain at 20 and 40% of the ultimate strain.

Standard deviations were calculated using the "total population" method (Pearson's method) in accordance with the AFGC guide recommendation (AFGC, 2021). These calculations were based on the results of three repeated tensile tests.

In the case of GFRP rebars, no significant evolution of tensile properties was observed after one year of exposure to ANL conditions at 20°C and 40°C. However, a notable decrease in strength was observed at 60°C for exposures exceeding 180 days (reduction by about 16% after a 1-year exposure). For CFRP rebars, a significant decrease in strength was observed during the first two months of exposure at 60°C. However, after this initial period, a recovery in strength was observed, and the strength values tended to stabilize around the initial values of the unaged specimens.

According to the AFGC guide (AFGC, 2021), the minimum recommended elastic modulus for GFRP rebar is 45 GPa, while for CFRP rebar, it is 120 GPa. In terms of tensile strength, the guide suggests

achieving strengths of 850 MPa for GFRPs and 1700 MPa for CFRPs, considering the same diameters as those tested in our study. Upon comparing these recommended values with the results obtained during the characterization of the rebars at different time intervals, we observe that even after one year of aging in the different ANL conditions, the strengths and elastic moduli of the tested rebars remain higher than the values recommended by the AFGC guide.

Table 2: Residual tensile properties of FRP rebars aged under ANL conditions

Sample designation	Ultimate load (kN)	Tensile strength (MPa)	Tensile elastic modulus (GPa)	Standard deviation on strength (MPa)	Standard deviation on elastic modulus (GPa)
GFRP (unaged)	88.6	1128.3	58.0	42.8	1.6
CFRP (unaged)	153.5	1954.5	145.3	61.6	5.6
30 days_20°C_GFRP	85.8	1092.3	56.6	75.3	0.8
60 days_20°C_GFRP	90.8	1156.2	56.0	27.1	1.5
90 days_20°C_GFRP	84.9	1080.6	56.7	12.9	1.3
180 days_20°C_GFRP	93.2	1187.1	55.9	13.5	0.4
360 days_20°C_GFRP	91.7	1168.1	57.0	19.2	1.0
30 days_40°C_GFRP	91.9	1169.6	57.9	27.0	1.0
60 days_40°C_GFRP	86.4	1100.3	56.4	83.6	1.3
90 days_40°C_GFRP	86.2	1097.1	57.2	52.7	1.2
180 days_40°C_GFRP	91.6	1166.4	57.0	34.3	1.1
360 days_40°C_GFRP	87.0	1107.6	57.1	5.7	1.3
30 days_60°C_GFRP	88.9	1132.0	57.4	11.6	1.7
60 days_60°C_GFRP	87.5	1114.2	57.1	14.4	0.2
90 days_60°C_GFRP	80.0	1018.4	56.0	27.7	1.2
180 days_60°C_GFRP	84.5	1076.4	57.7	24.9	0.9
360 days_60°C_GFRP	74.3	946.6	56.0	10.7	1.6
30 days_60°C_CFRP	160.6	2044.7	146.7	34.2	2.1
60 days_60°C_CFRP	142.5	1813.8	148.2	122.3	1.8
90 days_60°C_CFRP	151.2	1925.4	148.0	35.4	0.4
180 days_60°C_CGFRP	153.4	1953.6	147.0	54.2	3.0
360 days_60°C_CFRP	153.8	1958.5	147.8	81.9	3.6

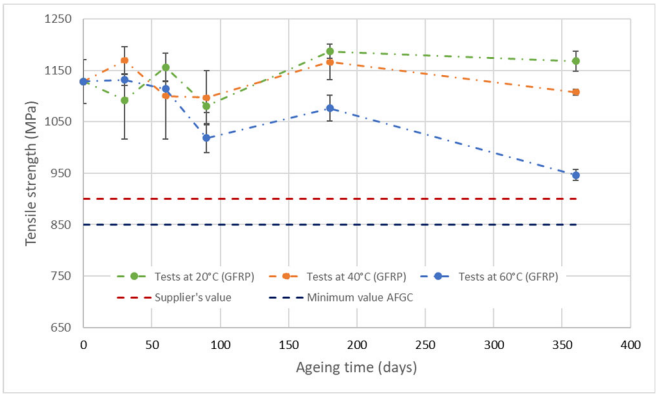

a) Tensile strength

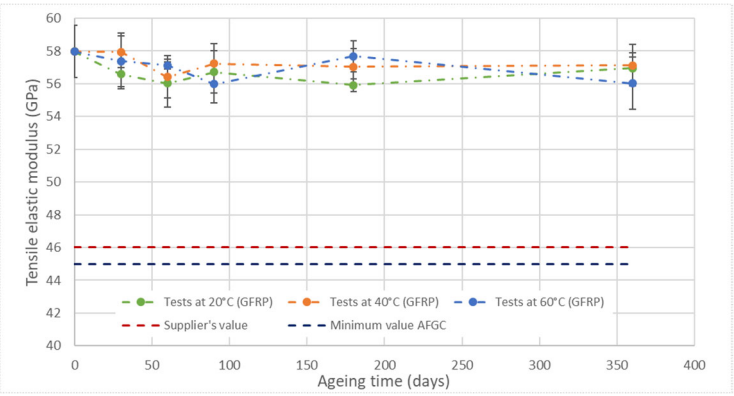

b) Elastic modulus

Figure 6: Evolution of the tensile properties of GFRP rebars during the aging process without load at different temperature (ANL conditions)

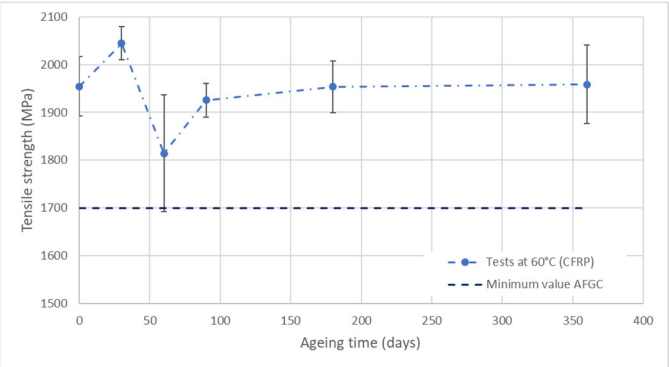

a) Tensile strength

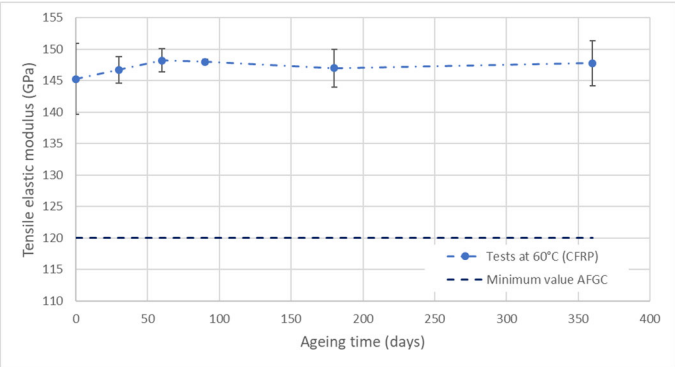

b) Elastic modulus

Figure 7 : Evolution of the tensile properties of CFRP rebars during the aging process without load (ANL) at 60°C.

Impact of ANL conditions on the interlaminar shear strength

Residual interlaminar properties of FRP specimens were evaluated through short-beam tests after exposure to ANL conditions. The observed failure mode for both GFRP and CFRP specimens was interlaminar fracture at the "neutral fiber," as illustrated in Figure 8.

a) GFRP rebar

b) CFRP rebar

Figure 8: Typical failure modes of ANL aged specimens after interlaminar shear test

The average Interlaminar Shear Strengths (ILSS) of the aged rebars are presented in Table 3, while their variations over time (at different temperatures for GFRPs and at 60°C only for CFRPs) are illustrated in Figure 9. The average values and standard deviations (Pearson) are calculated from the results of three repeated tests.

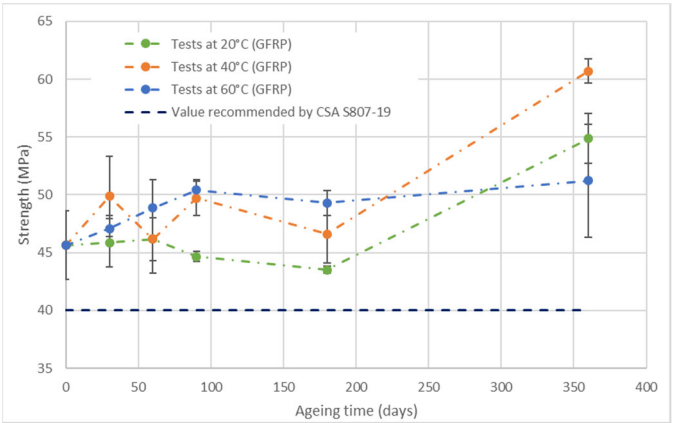

a) GFRP

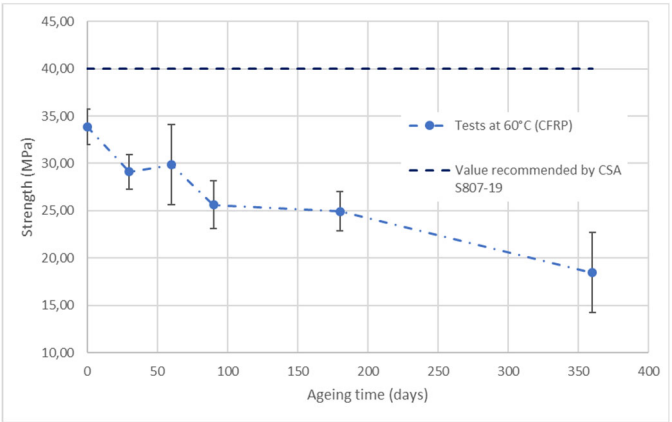

b) CFRP

Figure 9: Evolution of the interlaminar shear strength (ILSS) of GFRP (a) and CFRP (b) rebars during the aging process without load (ANL).

The results indicate an increase in interlaminar shear strength for GFRP rebars after 200 days of aging. Differently, for CFRP rebars, a significant decrease in ILSS is observed over aging at 60°C. Overall, the sensitivity to ANL aging appears to be higher for the matrix/carbon fiber interface compared to the matrix/glass fiber interface. This difference is likely attributed to the effectiveness of the sizing used (surface treatment of the fibers), which is generally better in the case of glass fibers.

According to the Canadian guide (CSA S807-19, 2010), a minimum ILSS value of 40 MPa is recommended for FRP rebars. It can be observed that initial values obtained for GFRPs are close to the guide's recommendations but still remain relatively low. On the other hand, the ILSS of CFRP rebars is significantly lower than the recommended values.

Table 3: Residual Interlaminar shear strength (ILSS) of FRP rebars aged under ANL conditions

Specimen designation	Strength (kN)	ILSS (MPa)	Standard deviation on ILSS (MPa)
GFRP (unaged)	5.4	45.7	3.0
CFRP (unaged)	4.0	33.9	1.9
30 days_20°C_GFRP	5.4	45.9	2.1
60 days_20°C_GFRP	5.4	46.2	2.9
90 days_20°C_GFRP	5.3	44.7	0.5
180 days_20°C_GFRP	5.1	43.5	0.3
360 days_20°C_GFRP	6.5	54.9	2.2
30 days_40°C_GFRP	5.9	49.9	3.5
60 days_40°C_GFRP	5.4	46.2	1.9
90 days_40°C_GFRP	5.9	49.7	1.5
180 days_40°C_GFRP	5.5	46.6	2.5
360 days_40°C_GFRP	7.1	60.7	1.1
30 days_60°C_GFRP	5.6	47.1	1.1
60 days_60°C_GFRP	5.8	48.9	2.5
90 days_60°C_GFRP	5.9	50.4	0.9
180 days_60°C_GFRP	5.8	49.3	1.1
360 days_60°C_GFRP	6.0	51.2	4.9
30 days_60°C_CFRP	3.4	29.1	1.8
60 days_60°C_CFRP	3.2	29.9	4.2
90 days_60°C_CFRP	3.0	25.6	2.5
180 days_60°C_CFRP	2.9	24.9	2.1
360 days_60°C_CFRP	2.2	18.5	4.2

Microstructural observations

Figure 10 presents optical microscopy images of polished cross sections of the reference GFRP and CFRP rebars.

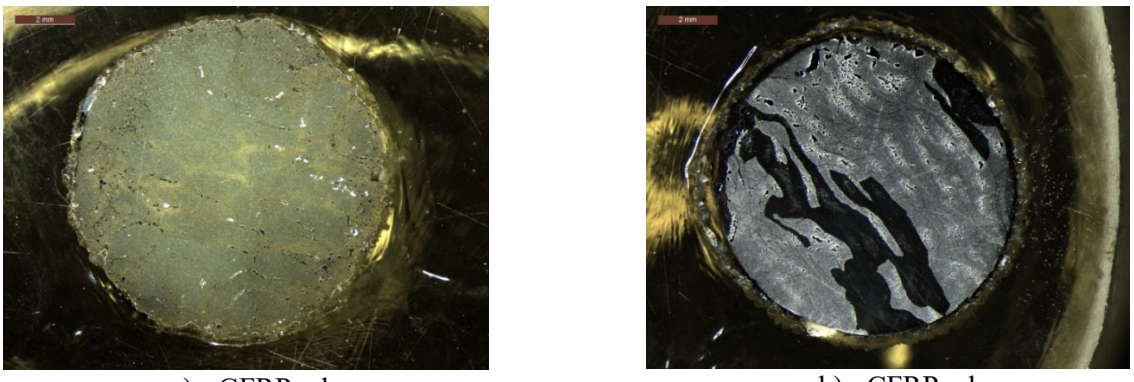

a) GFRP rebars b) CFRP rebar

Figure 10: Cross-sections of reference FRP specimens, as observed by optical microscopy

In the CFRP material, the presence of voids is prominently visible. These voids, which correspond to areas lacking matrix and/or fiber, lead to fiber sinking during the polishing process. Consequently, dark

regions can be observed on the cross-sections, indicating cavities with a difference in surface depth of approximately 10 µm. Similar observations were made on all CFRP samples (reference and aged). This high density of defects in CFRPs may provide an explanation for the degradation of interlaminar shear properties over ANL aging conditions, which was previously highlighted by short beam tests.

In contrast, the GFRP microstructure shows much lower defects (Figure 10 a), which is consistent with the better interlaminar shear behaviour under ANL aging.

Effect of ANL aging conditions on the glass transition temperature of the FRP rebars

Figure 11 shows the evolution of the glass transition temperature (Tg) for GFRP and CFRP specimens exposed to ANL aging conditions (embedment in concrete cylinders and immersion in the alkaline solution at selected temperatures) over periods of up to 1 year (365 days).

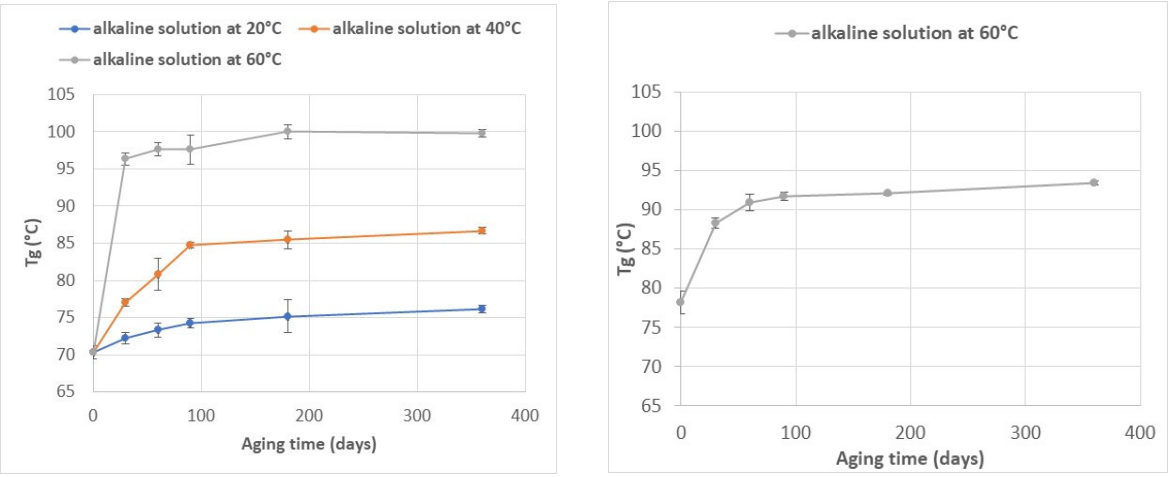

a) GFRP rebars b) CFRP rebars

Figure 11: Evolution of the Tg of GFRP and CFRP specimens during exposure to ANL aging conditions

The kinetics of Tg evolution of GFRP rebars is found to be highly influenced by the temperature of the aging solution. At 60°C, a rapid increase in Tg is observed, indicating a post-curing phenomenon. A similar post-curing process is observed at 40°C, but with slower kinetics. In contrast, at 20°C, the evolution of Tg is significantly slower, and even after 1 year of exposure, the polymerization of the vinylester matrix remains incomplete. Overall, these post-curing phenomena may explain the observed increase in interlaminar shear strength (ILSS) for GFRP rebars exposed to ANL conditions (Figure 9 a). In the case of CFRP rebars aged at 60°C, a rapid increase in Tg is also observed, which can be attributed to post-curing. However, this increase does not result in higher interlaminar shear strength (ILSS) values (Figure 9 b), indicating that interfacial degradation processes predominate over post-curing effects in CFRPs.

PRELIMINARY RESULTS UNDER ASL AGING CONDITIONS (WITH SUTAINED LOAD)

Effects of ASL aging on the tensile properties of GFRP s and comparison with ANL conditions

At this stage of the study, only a few GFRP specimens have been subjected to combined environmental and mechanical conditions (ASL). It is worth noting that some GFRP specimens, exposed to the most severe conditions (60°C/40% of the tensile strength and 40°C/40% of the tensile strength), experienced premature failure during the aging process after 12 and 70 days, respectively. These rebars were unable to undergo tension testing afterward, but they were later tested using short beam tests.

The residual tensile properties of the GFRP rebars that did not fail during ASL aging and could be tested afterward are presented in Table 4. Additionally, Figure 13 compares the tensile strengths of the GFRP specimens aged in ASL and ANL conditions (with and without combined load). The values of

specimens that failed prematurely during ASL aging are also plotted on the graph (they are taken as the level of sustained load applied to these samples and are displayed as square marks on the graph).

Overall, its observed that the application of load during aging has a significant impact on the residual strength of the rebars, as values obtained after ASL exposure are lower than those under ANL conditions. Furthermore, this effect is highly dependent on temperature: at a given level of sustained load, the higher the aging temperature, the greater the effect of the combined load on the residual strength of the GFRPs.

Table 4: Residual tensile properties of the GFRP rebars aged under ASL conditions

Sample designation	Ultimate load (kN)	Tensile strength (MPa)	Tensile modulus (GPa)	Standard deviation on strength (MPa)	Standard deviation on elastic modulus (GPa)
42 days_40°C_40%_GFRP	68.8	876.3	56.4	54.5	1.4
90 days_20°C_40%_GFRP	85.8	1091.9	57.4	9.0	0.6

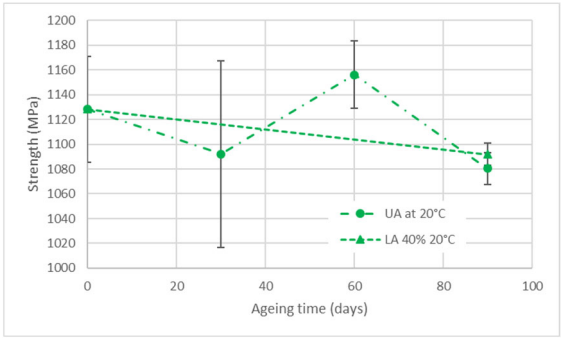

a) 20°C

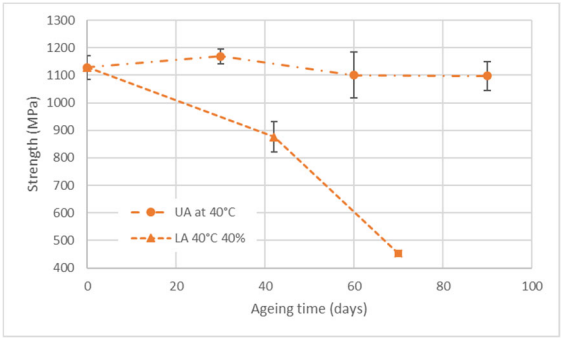

b) 40°C

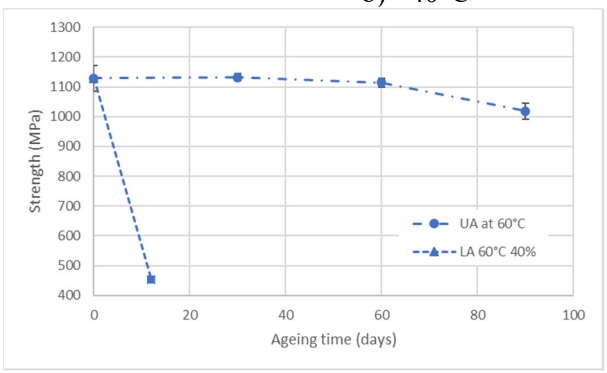

c) 60°C

Figure 12: Evolution of the residual tensile strength of GFRP rebars during ASL aging process (with combined load), and comparison with the evolution under ANL conditions (without load) at different temperatures.

Impact of ASL conditions on the interlaminar shear strength

This section focuses on the GFRPs aged under the ASL condition (60°C/40% of tensile strength) that experienced premature failure after 12 days of exposure during the aging process. Despite the failure occurring near the anchorages, portions of the rebars remained intact and could be subjected to short beam tests to evaluate their interlaminar properties.

The average ILSS value for this series of specimens is presented in Table 5. In Figure 13, a comparison is made between this ILSS value and the values obtained for specimens aged under ANL condition at the same temperature (60°C). Interestingly, the ILSS of the ASL-aged specimen is significantly higher, indicating that the combined environmental/mechanical aging process contributes to a substantial improvement in the fiber/matrix properties. However, the underlying mechanism responsible for this enhancement has not been identified at this stage.

Table 5: Residual Interlaminar shear strength (ILSS) of FRP rebars aged under ASL conditions

Specimen Designation	Ultimate load (kN)	ILSS (MPa)	Standard deviation on ILSS (MPa)
12 days_60°C_40%_GFRP	6.8	57.7	1.2

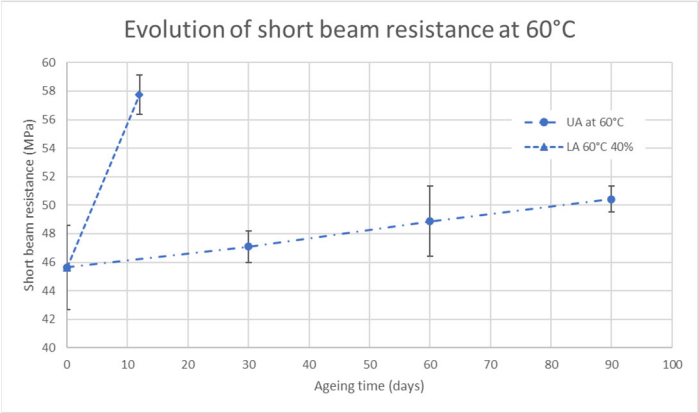

Figure 13: Evolution of the ILSS of GFRPs during ASL aging process at 60°C/40% of tensile strength and comparison with ANL results.

Microstructural observations

Figure 14 illustrates the cross sections of GFRP rebars that underwent aging under ASL conditions at 60°C/40% of the tensile strength. These rebars experienced premature failure after being exposed for 12 days; however, SEM (Scanning Electron Microscope) observations were conducted on the intact sections of the bars. These observations reveal numerous cracks in the core of the aged rebars. It appears that the failure path primarily occurs at the fiber/matrix interfaces, although damaged glass fibers are also observed. This failure mechanism, induced by sustained load, might have facilitated the penetration of alkaline solution into the rebars, thereby potentially accelerating the damage kinetics under the ASL condition. Complementary analyses using Energy-dispersive X-ray spectroscopy (EDX) are currently being conducted to assess whether alkali ions were able to penetrate into the core of the aged rebars.

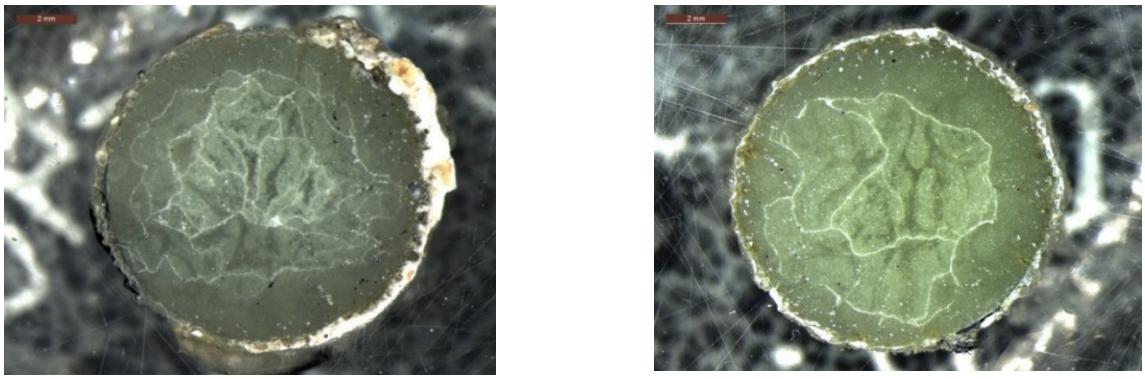

Figure 14: Optical microscopy images the cross-sections of GFRP rebars aged for 12 days under ASL conditions at 60°C/40% of the tensile strength.

CONCLUSION

An experimental program was conducted to investigate the durability of GFRP and CFRP rebars under pure environmental aging (ANL condition). The effect of combined environmental/mechanical aging (ASL condition) was also investigated, but only in the case of GFRPs. The comprehensive test program involved monitoring the evolution of residual mechanical properties of the aged rebars, through tensile and short-beam tests, as well as studying the evolution of relevant physico-chemical and microstructural properties. To ensure experimental efficiency, the design of experiments for the ASL conditions was optimized using the Hoke matrix concept.

The study revealed that ANL aging (without mechanical load) in an alkaline solution at various temperatures, had different effects for the GFRP and the CFRP rebars. In the case of GFRPs, the residual tensile properties were little affected by a 1-year exposure period, except at the temperature of 60°C where a 16% decrease in strength was observed. Interestingly, the interlaminar shear strength (ILSS) of GFRPs exhibited a significant improvement during ANL aging, likely attributable to the post-curing process of the polymer matrix, as evidenced by DSC experiments. Conversely, CFRP rebars demonstrated no significant change in tensile properties after 360 days of exposure at 60°C. However, the residual ILSS gradually decreased during aging under this condition, suggesting that degradation of the fiber/matrix interface prevails over post-curing effects for the studied CFRP rebars.

Regarding ASL aging of GFRP rebars, it was found that the sustained load had a substantial influence on the degradation kinetics of the rebar. The specimens subjected to ASL conditions exhibited lower residual tensile strengths compared to those exposed to ANL at the same temperature. This effect was temperature-dependent, with a more pronounced impact observed at higher aging temperatures. This phenomenon is potentially attributed to a failure process that takes place under high sustained load at elevated temperature, which promotes the penetration of alkaline solution into the GFRP rebar and accelerates the degradation of the glass fibers (to be confirmed through additional investigations). Conversely, it was observed that the ILSS of the GFRP rebars increased during ALS aging, but the mechanism behind this enhancement remains unidentified at this stage.

REFERENCES

Souchu, P. (2009). *La corrosion des armatures danger majeur pour la durabilité des ouvrages en béton armé*. http://doc.lerm.fr/

AFGC (2021). *Utilisation d'armatures composites (à fibres longues et à matrice organique) pour le béton armé.*

Byars, E.A., Waldron, P., Dejke, V., Demis, S., & Heddadin, S. (2003). Durability of FRP in concrete – deterioration mechanisms. *International Journal of Materials and Product Technology*, 19(1-2).

ASTM D7205/D7205M-06 (2006). *Standard test method for tensile properties of fiber reinforced polymer matrix composite bars*. American Society for Testing and Materials (ASTM). West Conshohocken. PA. USA.

ISO/AWI 10406-1 (2008). *Fibre-reinforcement polymer (FRP) reinforcement of concrete – Test methods*. Organisation Internationale de normalisation (ISO).

ASTM D4475-21 (2006). *Standard test method for apparent horizontal shear strength of pultruded reinforced plastic rods by the short-beam method. American Society for Testing and Materials (ASTM)*. West Conshohocken. PA. USA.

ASTM D4475-02 (2002*). Standard test method for apparent horizontal shear strength of pultruded reinforced plastic rods by the short-beam method*. American Society for Testing and Materials (ASTM). West Conshohocken. PA. USA.

Rolland, A., Benzarti, K., Quiertant, M., Chataigner, S. (2021). Accelerated Aging Behavior in Alkaline Environments of GFRP Reinforcing Bars and Their Bond with Concrete. *Materials*, 14, 5700. https://doi.org/10.3390/ma14195700

CSA-S807-19 (2019). *Spécification pour les polymères renforcés de fibres*. Canadian Standards Association. Mississauga. ON. Canada.

CONFLICT OF INTEREST

The authors declare that they have no conflicts of interest associated with the work presented in this paper.

DATA AVAILABILITY

Data on which this paper is based is available from the authors upon reasonable request.